Cyclotron Mode Frequency Shifts in Multi-species Ion Plasmas

M. Affolter, F. Anderegg, D. H. E. Dubin, and C. F. Driscoll
Department of Physics, University of California at San Diego, La Jolla, California 92093, USA
(Dated: October 9, 2013)

In trapped plasmas, electric fields and collective effects shift the cyclotron mode frequencies away from the "bare" cyclotron frequency for each species s. Here, these shifts are measured on a set of cyclotron modes ($m = 0, 1$, and 2) with $\cos(m\theta)$ azimuthal dependence in near rigid-rotor multi-species ion plasmas. We observe that these frequency shifts are dependent on the plasma density, through the $E \times B$ rotation frequency f_E, and on the "local" charge concentration δ_s of species s, in close agreement with theory.

Cyclotron mode frequencies are used in a broad range of devices to manipulate and diagnose charged particles. In trapped plasmas with a single sign of charge, collective effects and electric fields shift these cyclotron mode frequencies away from the "bare" cyclotron frequencies $2\pi F_c^{(s)} \equiv (q_s B/M_s c)$ for each species s, and collisions broaden the cyclotron resonances. These electric fields may arise from the trap potentials, from space charge, including collective effects, and from image charge in the trap walls. Modern high-throughput mass spectroscopy devices observe these frequency shifts [1–3], but typically use calibration equations that neglect collective effects [4] or conflate them with amplitude effects [2].

Here, we quantify cyclotron mode frequency shifts in well-controlled, laser-diagnosed, multi-species ion plasmas, with near uniform charge density n_0 characterized by the $E \times B$ rotation frequency $f_E \equiv cen_0/B$. These shifts are measured at small amplitudes for a set of cyclotron modes varying as $\cos(m\theta - 2\pi f_m t)$, including the first quantitative measurements of the rarely observed $m = 0$ cyclotron mode with no azimuthal dependence [5–7].

For radially uniform species densities $n_s(r)$, the measured frequency shifts corroborate a simple theory expression [8–10], in which collective effects enter only through f_E and through the species fractions $\delta_s \equiv n_s/n_0$. Absent laser diagnostics, the measured frequency shifts could then be used to determine f_E and δ_s. At ultra-low temperatures where centrifugal separation of masses becomes significant, we observe large frequency shifts, described by a more general theory involving a radial integral over $n_s(r)$, with a simple asymptote for complete separation.

The cylindrical ion plasmas are confined in a Penning-Malmberg trap with a magnetic field $B = 2.965 \pm 0.002$ Tesla. The ions are predominately Mg^+ resulting from a Magnesium electrode arc, with $5 - 30\%$ other ions, typically H_3O^+ and O_2^+, arising from background gas at a pressure $P \leq 10^{-9}$ Torr. Typical isotopic charge fractions are $\delta_{24} = 0.54$, $\delta_{25} = 0.09$, $\delta_{26} = 0.10$, with the remaining 27% a mixture of H_3O^+ and O_2^+.

The ions are confined for days in a near rigid-rotor equilibrium state, by use of a weak applied "rotating wall" (RW) field [11]. Altering the frequency of this RW field, the plasma can be arranged to a desired density and rotation frequency. The ion densities range over $n_0 = (1.8 \rightarrow 6.2) \times 10^7$ cm^{-3}, with rotation rates $f_E = (9 \rightarrow 30)$ kHz, and inversely varying radii $R_p = (6 \rightarrow 3)$ mm. The plasma length $L_p \sim 10$ cm and wall radius $R_w = 28.6$ mm remain fixed.

Laser cooling of the $^{24}Mg^+$ enables temperature control from $(10^{-5} \rightarrow 1)$ eV. For most measurements, the plasma is laser-cooled to $T \sim 10^{-2}$ eV, giving a small Debye length $\lambda_D \sim R_p/35$ and a near-uniform density profile. At this temperature the ion species are intermixed radially, with inter-species collisionality $\nu_{ii} \sim 10^3$ /sec. In contrast, plasmas at $T < 10^{-4}$ eV exhibit near-complete centrifugal separation of species [12–14].

Radial profiles of the plasma temperature, total Mg^+ density, and rotation velocities, $v_\theta(r)$, are obtained using Laser Induced Fluorescence (LIF) [15]. Figure 1 shows measured density and rotation profiles (symbols) at three different rotation rates. These profiles are a convolution of the true "top-hat" plasma profile with the finite size (half-width 0.39 mm) probe laser beam. The profiles are fit assuming a convolved "top-hat" rigid-rotor model with $n(r) = n_0$ and $v_\theta(r) = 2\pi r f_E$ for $r \leq R_p$, giving the dashed lines in Fig. 1. The solid lines in Fig. 1 represent the true "top-hat" Mg^+ density and rigid-rotor rotation profiles of the plasma resulting from this fitting process. This rigid-rotor rotation frequency f_E and "top-hat" radius R_p will be used to characterize the cyclotron mode frequency shifts.

The cyclotron resonance frequencies are detected using Thermal Cyclotron Spectroscopy (TCS). A series of RF bursts, scanned over frequency, are applied to azimuthal sections of a confinement ring. Resonant wave absorption causes plasma heating, which is either detected as an increase in the plasma temperature, or as a change in the cooling fluorescence. For short bursts near resonance for species s, the change in the plasma temperature is measured to be $\Delta T \propto \delta_s A_b^2 \tau_b^2 / M_s$; here A_b is the burst amplitude and τ_b is the burst period. The changes in temperature for different excited species can provide a measurement of the charge fractions δ_s.

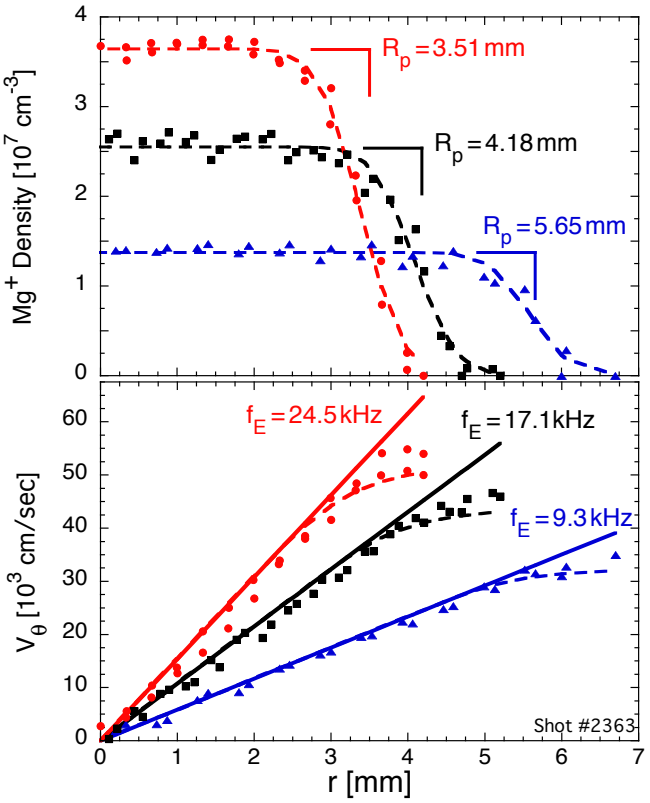

FIG. 1. (Color online) Radial profiles of Mg^+ density (Top) and rotation velocities (Bottom) at three different rotation rates in the "uniform density" temperature regime $T \sim 10^{-2}$ eV. Symbols are laser-width-averaged data, and dashed curves are fits to the "top-hat" rigid-rotor model (solid lines).

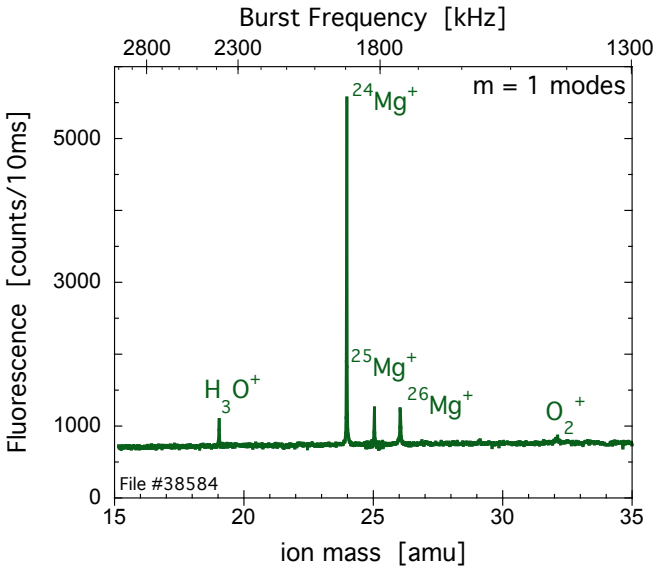

FIG. 2. (Color online) Mass spectra of a typical plasma containing $^{24}Mg^+$, $^{25}Mg^+$, and $^{26}Mg^+$; with H_3O^+ and O_2^+ impurity ions.

Here, we are interested in the frequency and natural width of these cyclotron resonances, so long bursts with narrow frequency widths are used. The sine-wave bursts consist of 10^4 cycles at $(0.1-3)$ V_{pp}, with $\pm$ polarity on sectors chosen as to give $\cos(m\theta)$ electric fields. These bursts typically heat the plasma by $\Delta T \lesssim 10^{-2}$ eV, which is observed as a change in the laser cooling fluorescence.

A typical broad $m = 1$ TCS scan is shown in Fig. 2. This TCS scan enables identification of the ion species, but the change in the cooling fluorescence (the height of the peaks in Fig. 2) suggests about 50% more $^{24}Mg^+$ than measured with LIF diagnostics. A possible cause for this discrepancy is that heat is directly removed from the laser cooled $^{24}Mg^+$, but only from the other species through collisions.

The center-of-mass $m = 1$ cyclotron mode is most commonly used for mass measurements, but other cyclotron modes exist and can provide further information on the plasma. Theoretical work [8–10] has predicted a set of cyclotron modes $m = 0, 1, 2, ...$ with $f_m^{(s)} \sim F_c^{(s)} + O(f_E)$. The $m = 2$ mode is a rotating elliptical surface perturbation, and the novel $m = 0$ mode is a radial "breathing" mode which generates no external electric field except at the plasma ends.

Figure 3 shows experimental observation of this set of azimuthal modes for $^{24}Mg^+$. Each mode is driven with the corresponding $\cos(m\theta)$ electric field. These modes are shifted away from the "bare" cyclotron frequency $F_c^{(24)} = 1899.22$ kHz, and have frequency spacing of approximately $f_E = 9.3$ kHz. The cyclotron mode frequencies are measured from the peaks in this heating response, and we note that the width of these resonances is a possible measurement of the mode damping γ.

Compressing the plasma with the RW increases f_E, enabling measurements of the cyclotron resonances under different space charge conditions on the same trapped ions. In Fig. 4 the cyclotron mode frequencies of the $m = 0, 1$, and 2 modes are plotted versus f_E for $^{24}Mg^+$, $^{25}Mg^+$, and $^{26}Mg^+$. The cyclotron mode frequency shifts are proportional to f_E, but the proportionality constants are different for the majority species $^{24}Mg^+$, than for the minority species $^{25}Mg^+$ and $^{26}Mg^+$, due to plasma collective effects.

These isotope-dependent frequency shifts can be understood from plasma wave theory. For a cold, *radially uniform* ion plasma with uniform rotation rate f_E and species concentration δ_s, theory [8–10] and simulations [16] predict that these modes are all frequency-shifted proportional to f_E, as

$$f_m^{(s)} - F_c^{(s)} = [(m-2) + \delta_s(1-\mathcal{R}_m)]\, f_E. \qquad (1)$$

The $\delta_s(1-\mathcal{R}_m)f_E$ term represents collective interactions in the plasma frame rotating at f_E; the $-2f_E$ term is the Coriolis force in the plasma frame; and the mf_E term is

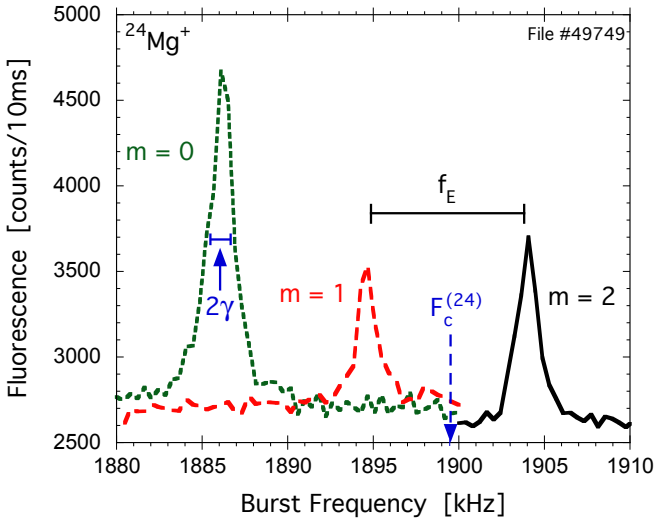

FIG. 3. (Color online) Measured cyclotron resonances at $T \sim 10^{-2}$ eV for $m = 0, 1$, and 2, shifted away from the "bare" cyclotron frequency $F_c^{(24)}$. These modes have a frequency spacing of approximately the $E \times B$ rotation frequency $f_E = 9.3$ kHz.

the Doppler shift back to the lab frame. For $m \geq 1$, the wall image charge correction is $\mathcal{R}_m \equiv (R_p/R_w)^{2m}$, but $\mathcal{R}_m \equiv 0$ for $m = 0$. The $\delta_s f_E = (f_p^{(s)})^2/2F_c^{(s)}$ shifts reflects plasma frequency f_p restoring forces, as seen in the upper-hybrid modes with $f_{uh}^2 = F_c^2 + f_p^2$.

Fitting Eq. 1 to the measured frequency shifts in Fig. 4, we find that the observed mode frequency spacing is consistent to within the 2% accuracy of the LIF measurements of f_E, and that these cyclotron modes converge to the "bare" cyclotron frequency $F_c^{(s)}$ in the limit $f_E \to 0$. Also, the slope of the frequency shifts in Fig. 4 provide a measurement of the charge fraction (i.e. density fraction) δ_s for each species. The relative Mg^+ ratios δ_{25}/δ_{24} and δ_{26}/δ_{24} are within 20% of those obtained through LIF diagnostics, and the corresponding mass ratios from $F_c^{(s)}$ are accurate to within 200 ppm.

Absent laser diagnostics, four frequencies from 2 m-theta modes in two plasma states could be used to determine the plasma characteristics f_E and δ_s, and thereby determine $F_c^{(s)}$. In Fig. 4, the measured cyclotron frequency differences of the two circled (vertical) data pairs give $f_E = (9.33, 16.97)$ kHz versus the measured $(9.29, 17.13)$ kHz; and Eq. 1 then gives $\delta_{26} = 9.06\%$ and $F_c^{(s)} = 1753.82$ kHz, in close agreement with the results in Fig. 4. Of course, similar information from multiple species would improve this plasma characterization.

In single-species plasmas ($\delta = 1$), the $m = 1$ mode is shifted only by the diocotron frequency $f_D = f_E\mathcal{R}_1$ [17], due to image charge in the conducting walls. In multi-species plasmas, the cyclotron mode frequencies are shifted by the total electric field, and by intra-species collective interactions. Prior multi-species work described

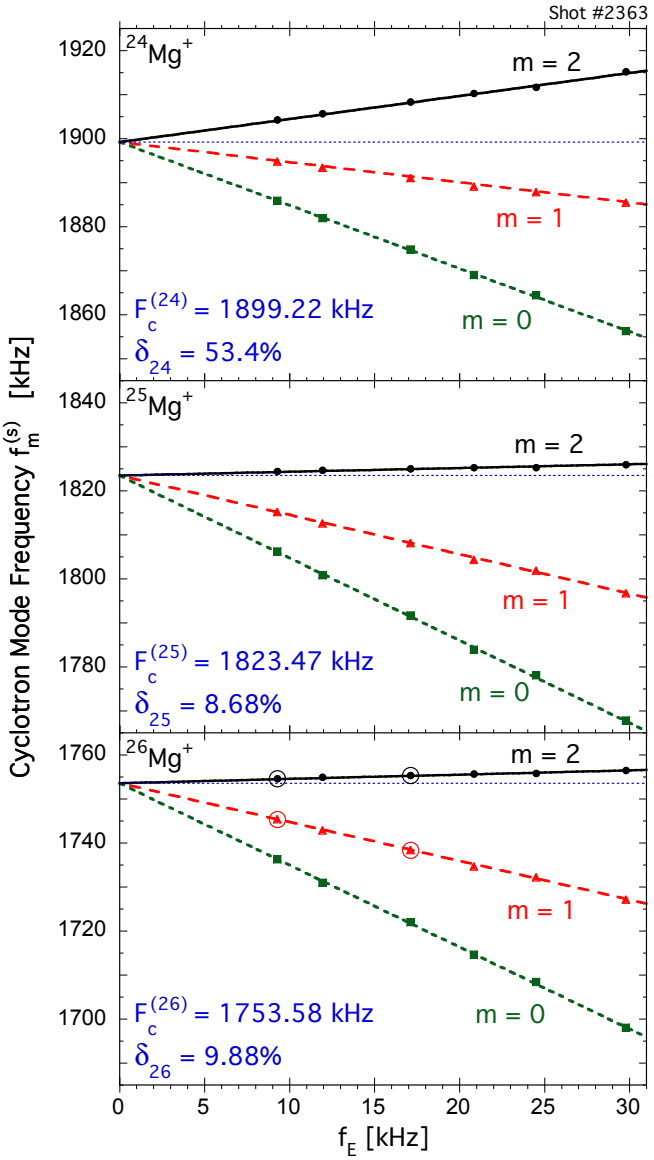

FIG. 4. (Color online) Cyclotron mode frequencies versus measured f_E for $^{24}Mg^+$, $^{25}Mg^+$, and $^{26}Mg^+$. Symbols are experimental data and curves are fits to Eq. 1, which determine $F_c^{(s)}$ (dotted) and δ_s for each species.

the spacing between the m-modes as several f_D [18] when image charges dominated, but in general, f_E is the more fundamental parameter, having little to do with R_w.

When the plasma is cooled to $T \lesssim 10^{-3}$ eV, ion species began to centrifugally separate by mass, and large unanticipated frequencies shift are observed. As shown in Fig. 5 for $^{24}Mg^+$, $^{26}Mg^+$, and H_3O^+ we observe that the center-of-mass mode frequencies shift towards the "bare" cyclotron frequency as the plasma is cooled. Similar temperature-dependent frequency shifts are observed for both the $m = 0$ and $m = 2$ modes, offset by $(m-1)f_E$.

For radially varying ion densities $n_s(r)$ or varying rotation $f_E(r)$, the mode resonances at $f_m^{(s)}$ are predicted [8]

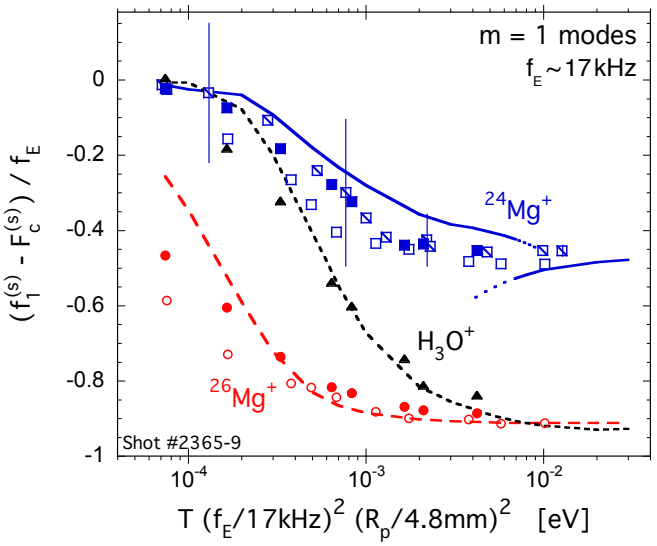

FIG. 5. (Color online) Normalized shifts of the $m = 1$ cyclotron mode frequencies for $^{24}Mg^+$, $^{26}Mg^+$, and H_3O^+, as the species centrifugally separate and concentrate radially. Symbol shapes represent species; symbol fill distinguishes measurements on 3 plasmas with slightly different compositions. The temperature T is scaled by the centrifugal energy of these plasmas, which differ by approximately 25%. Curves are theory predictions assuming a typical species concentration $M_s = (24, 25, 26, 19, 32)$ amu with $\delta_s = (54, 9, 9, 8, 20)\%$. The 4 vertical lines are the FWHM of the $^{24}Mg^+$ cyclotron resonace at various temperatures.

by peaks in the real part of the admittance $Re(Y_m)$. Here, $Y_m \equiv I/V$ relates electrode displacement current to electrode voltage. It has a frequency dependence of

$$Y_m \propto i(2\pi f)\frac{G_m + 1}{G_m - 1}, \tag{2}$$

with

$$G_m \equiv -\frac{2m}{R_w^{2m}}\int_0^{R_w} dr\,\frac{\beta(r)\,r^{2m-1}}{\alpha(r) - \beta(r)}, \tag{3}$$

$$\beta(r) \equiv \frac{n_s(r)}{n_0} f_E(0), \tag{4}$$

and

$$\alpha(r) \equiv (f_m^{(s)} - F_c^{(s)} + i\gamma/2\pi) - (m-2)f_E(r) + \frac{r}{2}\frac{\partial}{\partial r} f_E(r). \tag{5}$$

Peaks in $Re(Y_m)$ occur when $G_m \to 1$.

Numerically integrating Eq. 2 with $n_s(r)$ as predicted [12, 14] for centrifugal separation produces the theory curves in Fig. 5. As the plasma is cooled, the species centrifugally separate and concentrate into narrow radial annuli, increasing the "local" $n_s(r)$ towards the full "top-hat" density n_0. This increases the cyclotron frequency towards the single-species $\delta_s = 1$ limit. Here, the remaining shifts due to image charge [9] and trap electric fields are negligible. The discontinuity in the $^{24}Mg^+$ theory curve is due to multiple modes with different radial mode structure. Although multiple radial modes have been observed on some plasmas, they were not observed for this set of data, possibly due to stronger damping.

Varying the plasma temperature also changes the width of the cyclotron resonance, as shown by the "2γ" bars in Fig. 5. At high temperatures $T \gtrsim 10^{-2}$ eV, the resonance width is at least the frequency width of the drive, which is approximately 0.4 kHz. When the plasma is cooled, the ion-ion collision frequency increases, and the resonance width increases with the same qualitative behavior. For $T \lesssim 10^{-3}$ eV, inter-species collisions are reduced by centrifugal separation of the species, and at these temperatures the cyclotron resonance width is observed to remain constant at approximately 6 kHz.

At temperatures $T \gtrsim 0.1$ eV where ion-ion collisionality is small, we observed multiple closely-spaced modes with spacing dependent on T. This mode splitting is similar to that observed in electron plasmas [17]; but here this splitting occurs for the $m = 1$ mode which was not previously seen. Recent theory [9] involving radially standing Bernstein waves in multi-species ion plasmas predicts a similar frequency spacing, and a connection to this theory is being pursued.

For non-uniform total charge density $n(r)$ and non-uniform $f_E(r)$, Eqs. 2-5 predict strongly damped linear waves, in which the damping is caused by the variation in $f_E(r)$. In the case of a parabolic density profile, *i.e.* $n(r) = n_0(1 - ar^2)$, both theory and experiments [18] show that the peak of the $m = 1$ resonance occurs at frequencies well described by Eq. 1. In contrast, Eqs. 2-5 predict that the $m = 2$ mode frequencies are still proportional to f_E, but the constant of proportionality is approximately $0.25 + 0.5\delta_s$ rather than δ_s. These resonance widths are δ_s-dependent, with a typical FWHM of about $f_E/2$.

In summary, cyclotron mode frequencies on radially uniform ion plasmas are shown to shift by factors of the $E \times B$ rotation frequency f_E, as given by Eq. 1. Multiple azimuthal modes are observed, and measurements of these multiple mode frequencies can be used to determine f_E and δ_s. At low temperatures, centrifugal separation of species into radial annuli causes additional shifts of order f_E. In low collisionality regimes, cyclotron mode damping is weak, and multiple radial eigenmodes are possible.

This work was supported by National Science Foundation grant PHY-0903877, and Department of Energy grants DE-SC0002451 and DE-SC0008693.

[1] M. Easterling, T. Mize, and I. Amster, Analytical chemistry **71**, 624 (1999).
[2] C. Masselon, A. Tolmachev, G. Anderson, R. Harkewicz,

and R. Smith, Journal of the American Society for Mass Spectrometry **13**, 99 (2002).
[3] R. Wong and I. Amster, International journal of mass spectrometry **265**, 99 (2007).
[4] E. B. Ledford, D. L. Rempel, and M. L. Gross, Analytical Chemistry **56**, 2744 (1984).
[5] S. Barlow, J. Luine, and G. Dunn, International journal of mass spectrometry and ion processes **74**, 97 (1986).
[6] D. Rempel, E. Ledford Jr, S. Huang, and M. Gross, Analytical chemistry **59**, 2527 (1987).
[7] A. Peurrung, R. Kouzes, and S. Barlow, International journal of mass spectrometry and ion processes **157**, 39 (1996).
[8] R. W. Gould, Physics of Plasmas **2**, 1404 (1995).
[9] D. H. Dubin, Physics of Plasmas **20**, 042120 (2013).
[10] R. C. Davidson, *Physics of nonneutral plasmas*, Vol. 5 (Addison-Wesley New York, 1990) Chap. 5.6.1.
[11] F. Anderegg, E. Hollmann, and C. Driscoll, Physical Review Letters **81**, 4875 (1998).
[12] T. O'Neil, Physics of Fluids **24**, 1447 (1981).
[13] D. Larson, J. Bergquist, J. Bollinger, W. M. Itano, and D. Wineland, Physical review letters **57**, 70 (1986).
[14] G. Andresen, M. Ashkezari, M. Baquero-Ruiz, W. Bertsche, P. D. Bowe, E. Butler, C. Cesar, S. Chapman, M. Charlton, A. Deller, *et al.*, Physical review letters **106**, 145001 (2011).
[15] F. Anderegg, X.-P. Huang, E. Sarid, and C. F. Driscoll, Review of Scientific Instruments **68**, 2367 (1997).
[16] M. T. Nakata, G. W. Hart, and B. G. Peterson, Journal of the American Society for Mass Spectrometry **21**, 1712 (2010).
[17] R. W. Gould and M. A. LaPointe, Phys. Rev. Lett. **67**, 3685 (1991).
[18] E. Sarid, F. Anderegg, and C. F. Driscoll, Physics of Plasmas **2**, 2895 (1995).